Chemical Differentiation of Carbon Nanotubes in a Carbonaceous Matrix

Daniele Gozzi,*,† Alessandro Latini,† and Laura Lazzarini‡

Dipartimento di Chimica, SAPIENZA Università di Roma, Piazzale Aldo Moro 5, 00185 Roma, Italy, and IMEM-CNR, Parco Area delle Scienze 37/A, Localita' Fontanini, 43010 Parma, Italy

Received February 19, 2008. Revised Manuscript Received April 4, 2008

To determine the purity of carbon nanotubes (CNTs), the effectiveness of some inorganic substances to catalyze the Boudouard reaction, investigated by thermogravimetric experiments, was studied. The performance, in terms of ability to separate the feature of CNTs from the features of other components, of various catalyst powders (NiO, Rh, Cr_2O_3), thoroughly mixed with carbonaceous simulated mixtures, was checked under a pure CO_2 stream and compared without catalyst in the same operating conditions. The sequential removal of carbon up to 1200 °C by pure CO_2 from a real sample of MWCNTs was characterized by TEM, XRD, and micro-Raman spectroscopy the carbonaceous fraction residues at each stopping temperature. Some evidence of the poor reliability of Raman spectroscopy in detecting the CNT purity are discussed. The procedure to perform thermogravimetry of simulated mixtures under pure CO_2 at different weight compositions constituted by active carbon, MWCNTs, graphite, and Cr_2O_3 as catalyst was tested. The average relative error between the expected and found weight contents was within ±6%. The same procedure was also adopted to solve a simulated mixture of two kinds of MWCNTs having external diameter in a ratio of ∼1:10 and a very different number of walls.

Introduction

In the last 15 years or so since their discovery, carbon nanotubes (CNTs) have been playing a major role worldwide in research activities in so many areas of basic science[1] and technology because of their unique properties suitable for many current and potential applications.[2] Some materials containing CNTs are already on the market, though at present time the world production capacity is apparently quite limited. The figure of the effective capacity becomes decidedly reduced when nanotubes are selected for size, purity, number of walls, etc. The average price of 95% purity MWCNTs having selected distributions in diameter and length is still too high. This fact severely limits a diffuse utilization of MWCNTs for technological applications. One of the most interesting mass applications of MWCNTs is the fabrication of structural composite materials. As an example to evaluate the figures involved, it was found[3] that the performances of the concrete (improvements both in compressive strength, + 25 N/mm^2, and flexural strength, + 8 N/mm^2) were improved by addition of MWCNTs at the level of a few weight percent. Because of the high price of MWCNTs no high performance concrete with MWCNTs is on the market. A significant reduction of the MWCNT price would open a large market. To be conservative, suppose we utilized just 1 wt % MWCNTs in the high-performance concrete (HPC). HPC represents now 5% of the world production of concrete, which is estimated 1.6×10^9 ton/year.[4] This implies a potential world market of MWCNTs around 800 kton/year. There are other important mass applications such as the fabrication of tires, composite fibers, and electrical cables made of composite conductive fibers, etc., where MWCNTs could be utilized, provided that their price becomes competitive. The global market for carbon nanotubes will be worth $807.3 million by 2011. According to a new and updated technical market research report,[5] the global market for carbon nanotubes was $50.9 million in 2006 and is expected to grow up to $79.1 million by the end of 2007. At a compound annual growth rate (CAGR) of 73.8%, the market will reach $807.3 million by 2011.

The typology of the present and forecasted applications of CNTs depends even more strongly on their purity, and the attainment of a high level of purity is still a problem far from being solved.[6] The main sources of impurities are the residues of catalyst used and other carbonaceous species. The growth of CNTs requires the use of supported or unsupported catalysts that remain inevitably in the final product even after an accurate purification. This is due to the trapping of catalyst nanoparticles inside the CNTs, where the chemicals utilized for the catalyst removing cannot go in contact with them. Depending on the kind of catalyst utilized and synthesis conditions, the nucleation and growth of the CNTs can occur

* Corresponding author. E-mail: daniele.gozzi@uniroma1.it.
† SAPIENZA Università di Roma.
‡ IMEM-CNR.

(1) *Understanding Carbon Nanotubes*; Loiseau, A., Launois, P., Petit, P., Roche, S., Salvetat, J.-P., Eds.; Lectures Notes in Physics 677; Springer: Berlin, 2006.
(2) *Carbon Nanotubes Science and Applications*; Meyyappan, M., Ed.; CRC Press LLC: Boca Raton, FL, 2005.
(3) Italcementi Group. Presentation at the NanotechIT Meeting, Rome, Italy, June 21, 2007.
(4) *Nanotechnology and Construction*; Nanoforum: Düsseldorf, Germany, November 2006; http://www.nanoforum.org/.
(5) *Carbon Nanotubes: Technologies and Commercial Prospects*; Report NAN024C; BCC Research: Wellesley, MA, March 2007; www.bccresearch.com.
(6) Giles, J. *Nature* **2004**, *432*, 791.

10.1021/cm800484j CCC: $40.75
Published on Web 05/21/2008

by catalyst nanodusting, as in the case of unsupported catalysts,[7,8] and the final product is mainly constituted of CNTs having a catalyst nanoparticle attached at one of their ends. In this case, the removal of the catalyst can be almost complete.

Unfortunately, the carbon nucleation from the gaseous phase is never oriented only to the growth of CNTs; amorphous and/or graphitic carbon is simultaneously produced in some extent. Once the catalyst is fixed, this depends greatly on the synthesis temperature. The higher the temperature synthesis, the lower the amount of carbon formed as CNT carbon. Noncatalytic routes to MWCNTs (some types of the arc discharge and pulsed laser ablation deposition, PLAD, techniques, for instance) are also affected by the contamination from other carbonaceous forms. The same situation is normally found also in the synthesis of single-walled CNTs (SWCNTs).

One of the main tasks in qualifying the CNTs is the quantitative determination of the various forms of carbon present in a sample. The micro-Raman spectroscopy[9] (MRS) and thermogravimetry[10] (TG), along with differential thermogravimetry (DTG), are the techniques proposed in the literature. Transmission electron microscopy (TEM) always gives important support to both techniques.

As will be discussed later, MRS gives only qualitative information that rarely represents the real composition of the bulk sample and the capability to discriminate the various sp^2 forms of carbon is generally poor. TG and DTG have the potential to satisfy all of the requirements: quantitative, selective, accurate, and easy to manage. The composition of the gas phase and the presence of embedded or added catalysts to the sample are key factors to performing a successful and reproducible quantitative determination by TG of different CNT types together with other forms of carbon.

The scope of this work is to give a contribution in improving the purity determination in terms of carbon as CNT form by TG/DTG measurements of samples in a CO_2 atmosphere. To separate the feature of CNTs from other components, we performed the selection of a suitable catalyst to add to the carbonaceous mixture.

State of the Art

The first papers[11,12] dealing with the oxidative determination of CNTs in carbonaceous samples were published in 1993; in both cases, oxidation by air was performed. The capability of discriminating among various carbon forms is markedly reduced when pure oxygen or oxygen containing mixtures are used. This is due to the large exothermic effect caused by the combustion of any carbon form that activates almost simultaneously the reactions of all the carbonaceous species present in the sample. This fact has been reported by several authors,[10,13–15] and confirmed in the present work, as will be shown later. The reaction of CO_2 with a carbonaceous species, C_i, is very well-known as the Boudouard reaction

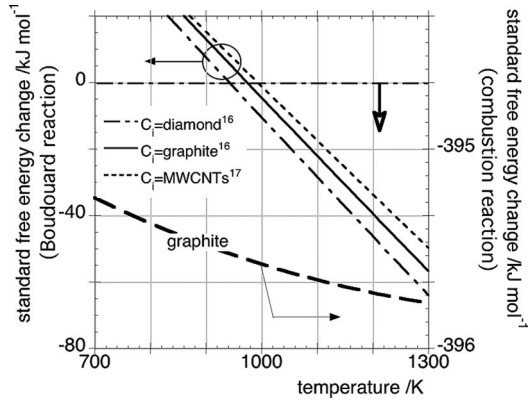

Figure 1. Standard free energy change against absolute temperature of (left scale) the Boudouard reaction (1) with different forms of carbon and (right scale) the combustion of graphite in pure oxygen.

$$C_i + CO_2(g) = 2CO(g) \quad (1)$$

The standard free energy change of this reaction for graphite[16] (reference state), diamond,[16] and MWCNTs[17] is plotted against temperature in Figure 1 and compared with the combustion of graphite. The average values of $\Delta rH°$ in the 600−1400 K range are, respectively, 171 ± 2 and -394.6 ± 0.5 kJ mol^{-1} with C_i = graphite. At the standard reference state, thermodynamics states that reaction 1 occurs only above a given temperature, whereas the combustion reaction is possible at any temperature. Because of possible consecutive kinetic activations, the positive value of enthalpy of reaction 1 is very useful in avoiding the process of overlapping when TG is carried out on samples containing more than one carbonaceous species. The carbon-gas reaction was extensively studied[18–20] and the kinetic model based on Langmuir-type adsorption is generally accepted. The rate-limiting step is the decomposition of the oxygen-containing species adsorbed on the carbon surface to evolve into the final gaseous products.[21] In the absence of suitable catalysts,

(7) Tomellini, M.; Gozzi, D.; Latini, A. *J. Phys. Chem. C* **2007**, *111*, 3266.
(8) Gozzi, D.; Latini, A. *Production of carbon nanotubes and hydrogen by thermal decomposition of methane*. Patent No. 05802229.4−2111-IT2005000587.
(9) Di Leo, R. A.; Landi, B. J.; Raffaelle, R. P. *J. Appl. Phys.* **2007**, *101*, 064307.
(10) Trigueiro, J. P. C.; Silva, G. G.; Lavall, R. L.; Furtado, C. A.; Oliveira, S.; Ferlauto, A. S.; Lacerda, R. G.; Ladeira, L. O.; Liu, J.-W.; Frost, R. L.; George, G. A. *J. Nanosci. Nanotechnol.* **2007**, *7*, 3477.
(11) Pang, L. S. K.; Saxby, J. D.; Chatfield, S. P. *J. Phys. Chem.* **1993**, *97*, 6941.
(12) Ajayan, P. M.; Ebbesen, T. W.; Ichihashi, T.; Iijima, S.; Tanigaki, K.; Hiura, H. *Nature* **1993**, *362*, 522.
(13) Kajiura, H.; Tsutsui, S.; Huang, H.; Murakami, Y. *Chem. Phys. Lett.* **2002**, *364*, 586.
(14) Hu, H.; Zhao, B.; Itkis, M. E.; Haddon, R. C. *J. Phys. Chem. B* **2003**, *107*, 13838.
(15) Bom, D.; Andrews, R.; Jacques, D.; Anthony, J.; Chen, B.; Meier, M. S.; Selegue, J. P. *Nano Lett.* **2002**, *2*, 615.
(16) Belov, G. V.; Iorish, V. S.; Yungman, V. S. *IVTANTHERMO for Windows: Database of Thermodynamic Properties of Individual Substances and Thermodynamic Modeling Software*, version 3.0; Glushko Thermocenter of Russian Academy of Sciences: Moscow, Russia, 2005.
(17) Gozzi, D.; Iervolino, M.; Latini, A. *J. Am. Chem. Soc.* **2007**, *129*, 10269.
(18) Walzer Jr., P. L. ; Rusinko Jr., F.; Austin, L. G. In *Advances in Catalysis*; Eley, D. D., Selwood, P. W., Weisz, P. B., Eds.; Academic Press: New York, 1959; Vol. 11.
(19) Johnson, J. L. In *Chemistry of Coal Utilization*, 2nd supplementary editiion; Elliott, M. A., Ed.; Wiley: New York, 1981; Vol. 2.
(20) Tomita, A. In *Encyclopedia of Surface and Colloid Science*; Hubbard, A., Ed.; Dekker: New York, 2001.
(21) Tomita, A. *Catal. Surv. Jpn.* **2001**, *5*, 17.

the release of CO in reaction 1 is slower than the release of CO_2 in the case of the combustion. Therefore, on a thermodynamic basis, although reaction 1 is expected to work better for differentiating mixtures of carbonaceous materials, on a kinetic basis, the hindered release of CO from the surface reduces the possibility of discriminating the various species in a TG experiment. The catalysis of the Boudouard reaction drew interest[22,23] because several industrial processes involve CO_2 to remove carbon from deactivated catalysts; produce activated carbon, coal-fired power generation, and steel making in a blast furnace; and avoid undesirable reactions in carbon-based nuclear fuels, etc. Various mechanisms have been proposed for the catalyzed Boudouard reaction, and in the case of the metal-catalyzed reaction, the most adopted mechanism is the "spill-over" mechanism.[24] The chemisorption with dissociation of molecular oxygen on the metal catalyst surface is followed by migration of oxygen atoms to nearby carbon substrate, and CO formation takes place on the carbon surface. Another well-known mechanism is the "carbon-dissolution" mechanism, which is especially favored in the case of nickel catalysts. Dissolved carbon in nickel is more reactive than original carbon.[25]

The information reported in the literature on the catalyzed Boudouard reaction have been utilized in the present work and applied to the not yet solved problem of determining CNTs in a carbonaceous sample. This was done first in CNT synthetic samples by using TEM and MRS for the sequential identification of carbonaceous species removed selectively by CO_2 treatment, and then by looking for the best catalyst to differentiate CNTs when they, as pure material, are arbitrarily mixed with other carbon forms.

Experimental Section

(a) Materials. Graphite powder (synthetic, 1−2 μm) and activated carbon (Norit RB 10.6 pellets) were purchased from Aldrich; Cr_2O_3 (325 mesh, 99.7%) from Cerac; Rh (>99%) from Engelhard. NiO was prepared by calcination at 600 °C of $Ni(NO_3)_2 \cdot 6H_2O$ (Aldrich). Three types of MWCNTs were prepared by thermal decomposition of methane (Rivoira, 99.95% purity) on three different catalysts. Two of these catalysts were unsupported ball-milled $NdNi_5$ and Nd_2Fe_{17} intermetallic compounds. These compounds were synthesized by electron beam melting in high vacuum of pressed pellets made of the appropriate amounts of powders of the constituent elements.[26] Ni (100 mesh, 99.99%) was purchased from Aldrich; iron (150 μm, 99.9%) from Merck; neodymium (40 mesh, 99.9%) from Chempur. After the synthesis, the intermetallics were ball-milled overnight in a steel jar. The third catalyst used was a dispersion of 1:1 (atomic ratio) Fe−Co alloy nanoparticles on silica aerogel (10% of Fe+Co by weight). The details of its preparation are given elsewhere.[27] Methane decomposition was operated at 500 °C in the case of $NdNi_5$, and at 600 °C for Nd_2Fe_{17} and for the aerogel supported catalyst. The details of the apparatus utilized for CNTs synthesis is reported in literature.[7] In all cases, the catalysts were heated to the operating temperature in a stream of Ar (99.9995%), and Ar was then substituted by methane. The flow rate of methane in all experiments was 5 sccm (cm^3/min @ STP). MWCNT samples obtained from $NdNi_5$ and Nd_2Fe_{17} were purified from the catalyst by repeated hot 1:1 HCl treatments. In the case of CNTs prepared with aerogel catalyst, they were purified by a first treatment in hot 10 M NaOH to dissolve the silica matrix, followed by hot 1:1 HCl treatments to remove Fe and Co. TG in pure O_2, as reported in Figure 2, determined the impurity content of all the carbonaceous materials used in this work. In the case of CNTs, the residue is constituted by traces in the form of oxidized species of catalyst, which was used for their growth. This aspect will be treated in detail later on for MWCNTs grown on Nd_2Fe_{17}. The purity of carbon dioxide and oxygen used during TG experiments was, respectively, 99.998 and 99.999%.

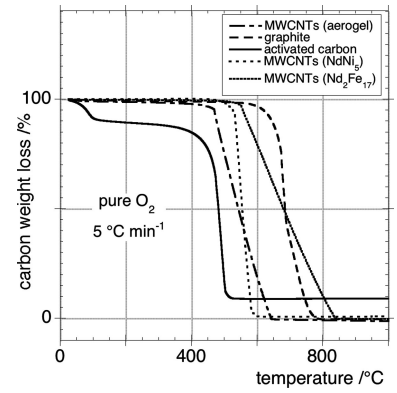

Figure 2. Carbon weight loss in pure oxygen of all the carbonaceous phases utilized in the present work.

(b) Thermogravimetry. Thermogravimetric measurements were performed by a Netzsch STA 409 PC Luxx thermobalance (temperature range: RT to 1500 °C; resolution: 2 μg) in simultaneous DTA-TG mode. Temperature was measured by means of a S-type thermocouple (Pt−Pt/Rh 10%). The thermocouple was calibrated against the melting points of In, Sn, Bi, Zn, Al, Ag, Au and Ni. All the measurements were performed in alumina crucibles. The CO_2 flow rate used in the experiments was 42 sccm. A correction measurement without sample was performed and subtracted to the TG and DTG curves of the samples.

(c) Transmission electron microscopy. TEM images were acquired with a JEOL 2000FX transmission electron microscope operating at 200 kV (source, LaB_6; resolution, 0.28 nm). Samples for imaging were prepared by ultrasonic dispersion of small amounts of powders in isopropanol and then putting a drop of the dispersion on carbon-coated copper grids.

(d) XRD. X-ray diffraction patterns were acquired using a Panalytical X'Pert Pro diffractometer (Bragg−Brentano geometry, radiation Cu Kα1, λ=0.154056 nm) equipped with a gas filled proportional detector. The Kβ radiation was cut by a Ni filter, while the Kα2 contribution to the obtained pattern was removed using the diffractometer software.

(e) Micro-Raman Spectroscopy. The samples were characterized by making use of a Renishaw inVia Raman Microscope (UK) equipped with Ar laser (λ = 514.5 nm, Ar^+).

Results

(1) (TG comparison in Different Conditions of a Simulated Sample of CNTs. Figure 3A shows the DTG behavior of a same sample of simulated mixture carried out in pure O_2, pure CO_2, and pure CO_2 with the addition of

(22) Walzer, P. L., Jr.; Shelef, M.; Anderson, R. A. In *Chemistry and Physics of Carbon*; Walzer, P. L., Jr., Ed.; Dekker: New York, 1968; Vol. 4.
(23) McKee, D. W. In *Chemistry and Physics of Carbon*; Walzer, P. L., Jr., Trower, P. A., Eds; Dekker: New York, 1981; Vol. 16.
(24) Tomita, A.; Tamai, Y. *J. Catal.* **1972**, *27*, 293.
(25) Trimm, D. L. *Catal. Rev. Sci. Eng.* **1977**, *16*, 155.
(26) Latini, A.; Di Pascasio, F.; Gozzi, D. *J. Alloys Compd.* **2002**, *346*, 311.
(27) Casu, A.; Casula, M. F.; Corrias, A.; Falqui, A.; Loche, D.; Marras, S.; Sangregorio, C. *Phys. Chem. Chem. Phys.* **2008**, *10*, 1043.

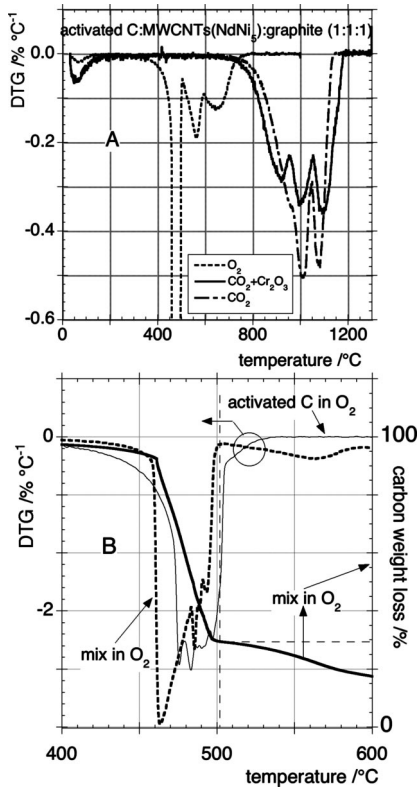

Figure 3. Thermogravimetry of a simulated mixture comprising activated carbon, MWCNTs grown on $NdNi_5$, and graphite in a 1:1:1 weight ratio at 1 °C min^{-1}. Comparison of the behavior in different environments: pure O_2, pure CO_2, and sample thoroughly mixed with Cr_2O_3 in pure CO_2. (A) DTG; (B) comparison between the thermogravimetry in pure O_2 of activated carbon and a 1:1:1 mixture in the temperature range where the intense DTG feature of panel A is displayed. (Left scale) DTG of the mixture and activated carbon; (right scale) carbon weight loss of the mixture.

Cr_2O_3 to the sample. The mixture comprises activated carbon, MWCNTs synthesized using $NdNi_5$[8] as catalyst, and graphite in a 1:1:1 weight ratio. To perform a correct comparison, we normalized the DTG curve of the sample with Cr_2O_3 to the total weight of carbon. The most intense DTG peak of the curve in pure O_2 is compared in Figure 3B with the DTG curve of a sample made of activated carbon only and burned in O_2. It is displayed in the right scale of the same plot as the corresponding TG curve of the mixture in O_2. Though the content of activated carbon in the mixture is 33 wt %, the corresponding weight loss is ~70 wt %. This implies that other species react almost simultaneously with activated carbon. It is evident that the TG performed under CO_2 gives a better resolution, which becomes decidedly higher when the sample is thoroughly mixed with the catalyst.

(2) Identification Procedure of Carbonaceous Species in a Synthetic MWCNT Sample. Figure 4 shows the TG and DTG curves obtained in CO_2 on a sample of MWCNTs synthesized under methane by utilizing Nd_2Fe_{17}[28] powder as unsupported catalyst. Three different phases, C_A, C_B, and C_C, have to be identified. To do this, two other distinct TG runs should be performed on the original sample by stopping each run of the temperature ramp at values T_A and T_B. At T_A, C_A has been removed, and at T_B, both C_A and C_B have

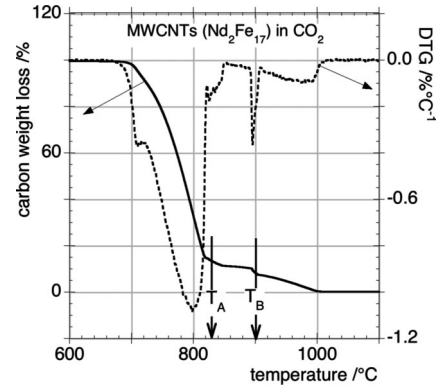

Figure 4. Thermogravimetry at 1 °C min^{-1} in pure CO_2 of MWCNTs grown on Nd_2Fe_{17}. Temperatures T_A and T_B are the stopping temperatures at which fractions S_1 and S_2 were selected. (Left scale) Carbon weight loss; (right scale) DTG.

been eliminated from the sample. At this point, the residue is constituted by C_C only. Therefore, to this end, three different samples, S_i, should be examined: $S_0 = C_A + C_B + C_C$ (the original one), $S_1 = C_B + C_C$, and $S_2 = C_C$. The TEM photos of the above S_i samples are reported in Figure 5 and the respective MRS spectra in Figure 6.

It is worth noticing that the TG curve in Figure 4 shows a good separation of the carbonaceous components even if no catalyst was added to the sample. This is explained by the presence of Nd_2Fe_{17} catalyst though the chemical removal of the catalyst after the synthesis. Because of a nucleation and growth process,[29] which shows differences from the mechanism proposed in the literature[7] when $NdNi_5$[8] is the catalyst of the MWCNT synthesis, some nanoparticles remain partially embedded in the growing MWCNTs and in the S_2 fraction. This represents an almost ideal dispersion of a catalyst, the activity of which becomes high even if its content is undetectable by TG (see Figure 4), whereas it is clearly detectable by XRD (see Figure 7) through the oxidized species found in the S_2 fraction by means of the comparison with XRD database.[30] By Powdercell software analysis of the diffraction pattern, the estimated catalyst content in S_0 is expected to be less than 1 wt %.

(3) Choice of the Best Catalyst. According to literature several substances can properly catalyze the Boudouard reaction: alkali carbonates,[31,32] transition metals, their oxides.[33,34] For the present task, the catalyst to add to the CNT sample should have some basic requirements: (*a*) no weight change in the TG operative conditions; (*b*) no solid-state reaction with the carbon matrix; (*c*) easy to manage without any particular precaution; (*d*) available as a very fine powder. A certain number of substances may match the above requirements. Three of them have been tested: Cr_2O_3, NiO, and Rh. The first two were recently studied[35] over the temperature range 850−1100 °C specifically for the catalyzed gasification kinetics of carbon by CO_2. Rh was tested because

(28) Gozzi, D.; Iervolino, M.; Latini, A. *J. Chem. Eng. Data* **2007**, *52*, 2350.
(29) Gozzi, D.; Latini, A.; Tomellini, M. Paper in preparation.
(30) JCPDS, International Centre for Diffraction Data, 2001.
(31) Rao, Y. K.; Han, H. G. *Ironmaking Steelmaking* **1984**, *11*, 308.
(32) Kapteijn, F.; Peer, O.; Moulijn, J. A. *Fuel* **1986**, *65*, 1371.
(33) Rankin, W. J. *Metall. Trans.* **1979**, *88C*, 107.
(34) Jagtap, S.; Kale, B.; Gokarn, A. *Metall. Trans.* **1992**, *23B*, 93.
(35) Karatas, C., *Miner. Process Extr. Metall. (Trans. Inst. Min. Metall., Sect. C)*, 2004, *113*, C19.

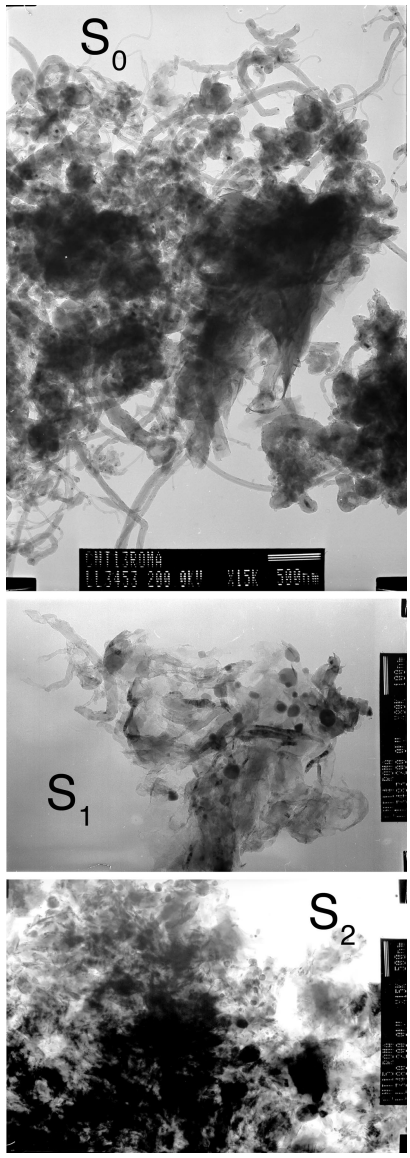

Figure 5. TEM photos of initial sample S_0 and fractions S_1 and S_2 obtained from the thermogravimetry of Figure 4.

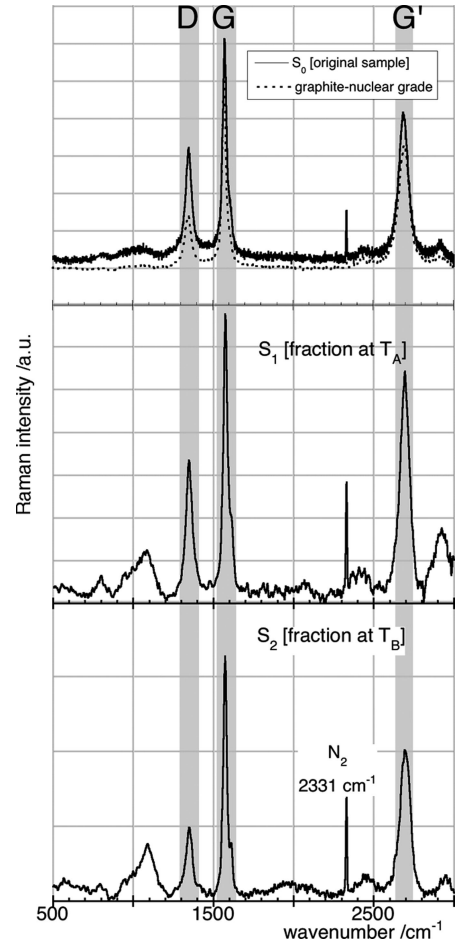

Figure 6. Micro-Raman spectra (Ar^+ laser at 514.5 nm) of the initial sample S_0 and fractions S_1 and S_2 obtained from the thermogravimetry of Figure 4. The line at 2331 cm^{-1} is the line of air N_2. The features other than D, G, and G′ bands should be attributed to the oxidation products of Nd_2Fe_{17} catalyst. The ratios between D, G, and G′ band intensities are reported in Table 3

it is a typical oxidation catalyst. Figure 8A shows the TG curves in pure CO_2 of simulated mixtures the composition of which is given in Table 1. The respective DTG curves are plotted in panel B of the same figure. The insert refers to the sample with catalyst NiO. Both TG and DTG curves are normalized with respect to the total weight of carbon with the exception of the curves performed without catalyst. NiO makes the Boudouard reaction so fast that no reliable resolution of the mixture components is possible. The anomalous behavior found with NiO will be treated in the discussion section. Though Rh shows a different behavior from NiO, in this case also, the resolution is not satisfactory. Cr_2O_3 works properly and its behavior was studied in detail.

(4) Simulated Samples of CNTs with Cr_2O_3 as Catalyst. The TG and DTG behavior in pure CO_2 with Cr_2O_3 and without catalyst are reported in Figure 9 for all the pure components (activated carbon, MWCNTs ($NdNi_5$), MWCNTs (aerogel), graphite) used to prepare the simulated mixtures. To allow a correct comparison between the curves, the data of the experiments with catalyst were all normalized to the total carbon weight loss (CWLN). Throughout Figure 9 Cr_2O_3 and carbonaceous materials were mixed to ensure a Cr_2O_3/C weight ratio close to 3. The averaged value was 2.9.

To test the ability of Cr_2O_3 to perform a reliable differentiation of CNTs in a carbonaceous matrix, some mixtures were prepared by mixing the MWCNTs, synthesized by $NdNi_5$ catalyst, each time with a different weight ratio combination of graphite and activated carbon. Figure 10 shows 4 panels that display the TG (left scale) and DTG (right scale) behaviors with and without catalyst. In each panel, it is also reported the CWLN TG curve. The initial weight percent compositions of each mixture are given in Table. 2, together with the weight ratio between Cr_2O_3 and total carbon in each sample. In the same table, the weight content found for each component of the mixture and the experimental total weight loss are also reported. The way by which the compositions were taken up from the experimental curves is displayed in the same figure by following the dashed lines. The points localized on each DTG curve and corresponding points on the CWLN TG curve define the related carbon weight loss, i.e., the component content in the mixture. The measured contents displayed in Figure

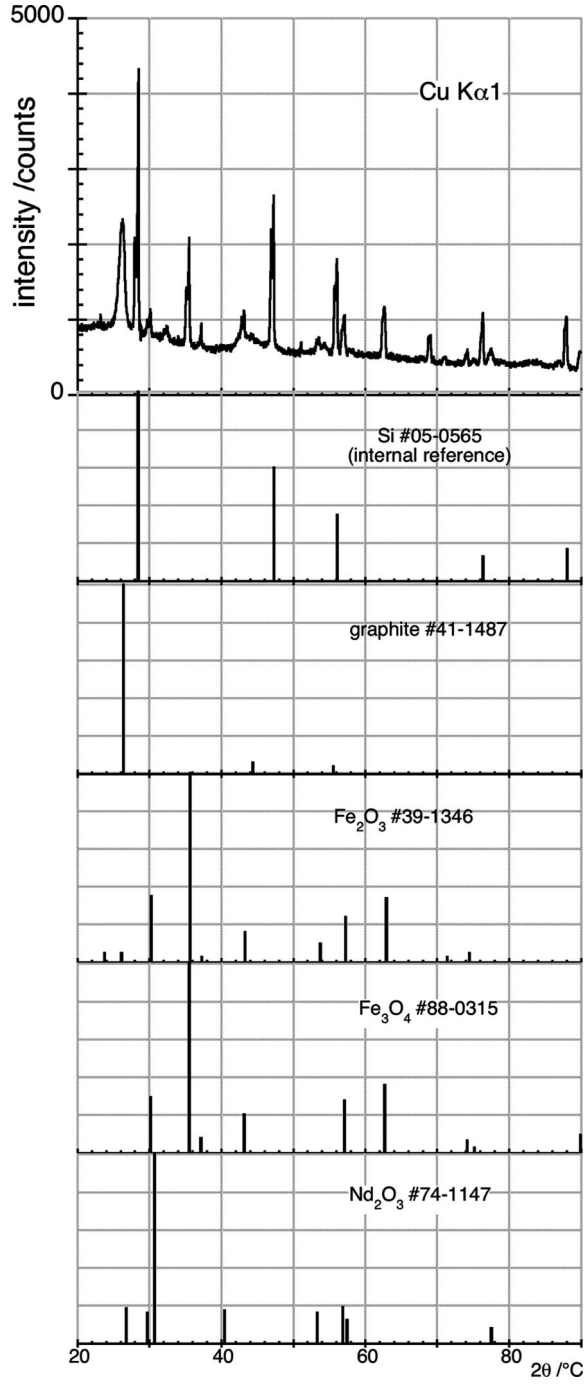

Figure 7. XRD spectrum of S_2 fraction obtained from the thermogravimetry of Figure 4. The features of graphite and oxidation products of Nd_2Fe_{17} are present. The lines of Si are also present and were intentionally added for 2θ internal reference reasons.

10 should be normalized to 100 because they are computed starting from the weight loss of activated carbon impurities at temperatures around 100 °C (see inset in the activated carbon panel of Figure 9).

The behavior of a simulated mixture constituted by two kinds of MWCNTs (synthesized using $NdNi_5$ and Fe−Co aerogel catalysts respectively) is reported in Figure 11. The two vertical gray strips refer to the DTG minima of the corresponding curve of the pure samples shown in Figure 9. Figure 12 demonstrates that the chosen samples of MWCNTs are different in both diameter and number of walls. MWCNTs in panel A are those synthesized using $NdNi_5$ as catalyst and their average diameter

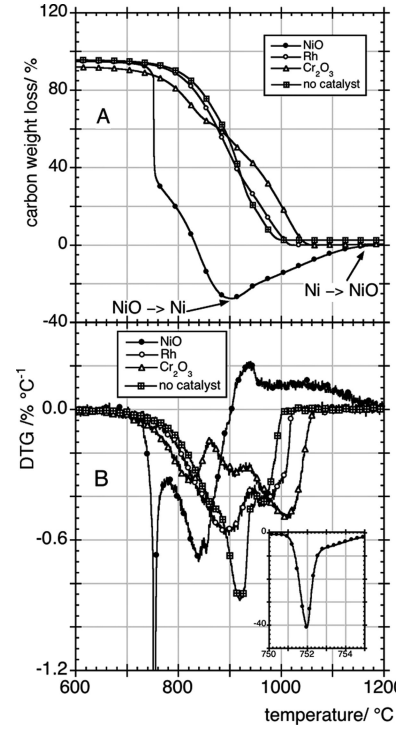

Figure 8. Thermogravimetry at 1 °C min^{-1} in pure CO_2 of simulated mixtures thoroughly mixed with different catalysts and without catalyst. The initial carbon composition with respect to the total carbon content of each mixture is reported in Table 1 (A) Carbon weight loss normalized to the total carbon weight loss; (B) DTG normalized to the total carbon weight loss. The inset shows the detail of DTG peak in the case of NiO catalyst.

Table 1. Initial Composition of the Mixtures of Figure 8

catalyst	activated C (%)	MWCNTs[a] (%)	graphite (%)	$W_{catalyst}/W_{total\ carbon}$
	32.0	46.7	21.3	0
Cr_2O_3	31.9	21.3	46.8	3.4
Rh	33.3	33.3	33.3	2.0
NiO	33.3	33.3	33.3	2.2

[a] Synthesized by $NdNi_5$ catalyst.[8]

is about an order of magnitude larger than the MWCNTs in panel B. The data coming from the graphical evaluation performed on Figure 11 are given in Table 2.

Discussion

The trends shown in Figure 4 refer to a real sample where we know[29] that the nucleation and growth of MWCNTs occurs together the formation of a not negligible quantity of other carbonaceous phases. Also, very defective MWCNTs should be considered embedded in these phases. Before discussing the above results, it is necessary to stress the point that it is practically impossible to drive a synthesis of CNTs without the simultaneous formation of a multiplicity of carbonaceous phases and with a sharp size distribution of CNT diameter and length. Therefore, the study of simulated mixtures appears the most practicable way to find the right procedure to catch information on how to proceed to identify and quantify CNTs in a real sample. On the other hand, simulated mixtures and real samples differ by several aspects. One of the most relevant is that a given component of the mixture can be different for structure, defectivity, particle

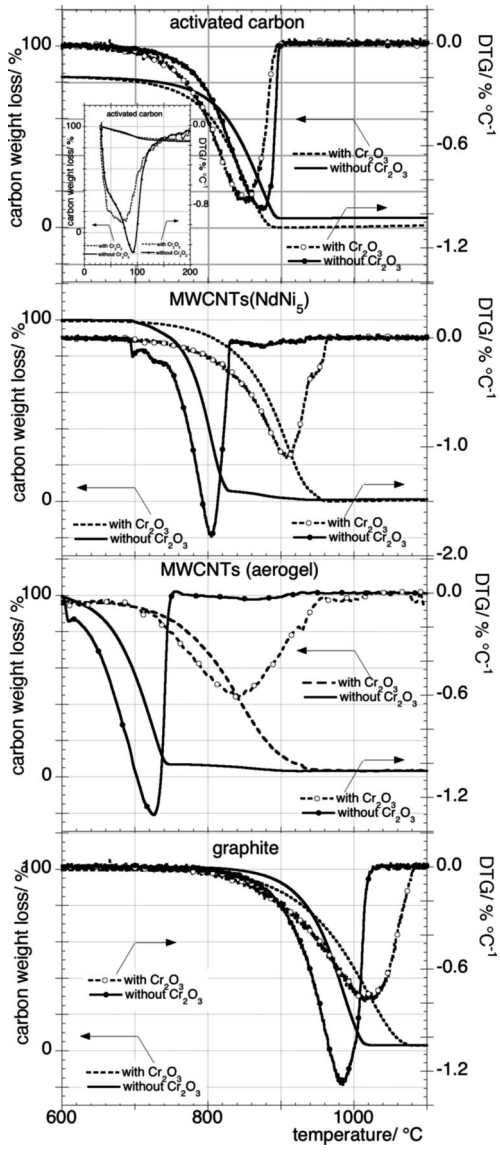

Figure 9. Thermogravimetry at 1 °C min^{-1} in pure CO_2 with and without Cr_2O_3 of each carbonaceous component of the simulated mixtures. The inset in the activated carbon panel displays the thermogravimetry behavior in the temperature range from RT to 200 °C. (Left scale) Carbon weight loss normalized to the total carbon weight loss; (right scale) DTG normalized to the total carbon weight loss.

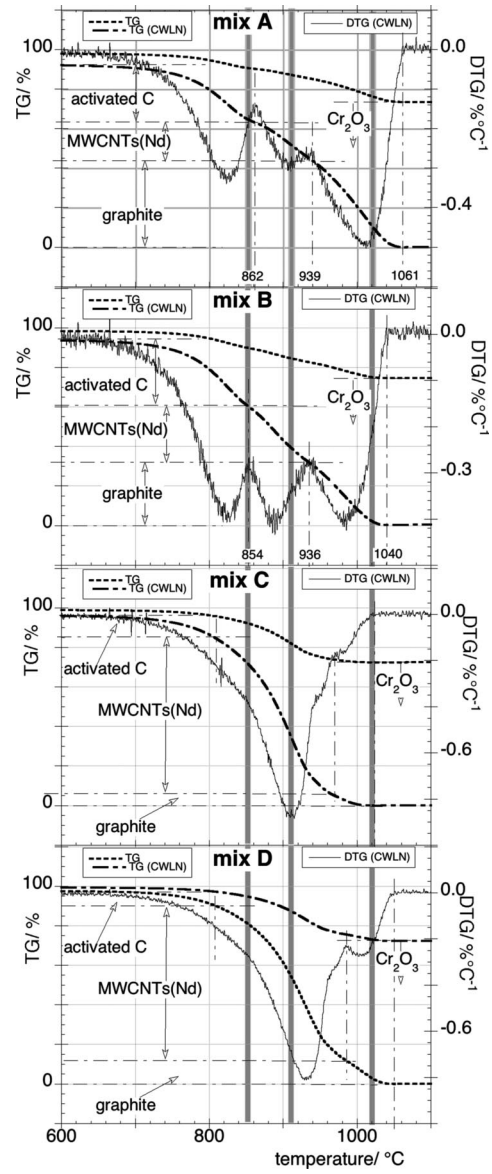

Figure 10. Thermogravimetry of 4 simulated mixtures comprising activated carbon, MWCNTs ($NdNi_5$), and graphite at 1 °C min^{-1} in pure CO_2 with catalyst Cr_2O_3. The initial and found compositions are given in Table 2 together with the experimental total carbon weight loss and the weight ratio between catalyst and carbonaceous mixture. In each panel is shown by dashed lines the graphic procedure to measure the weight contents. The three vertical grey strips each refer to the corresponding DTG minimum of the pure component when tested mixed with Cr_2O_3, as reported in Figure 9. (Left scale) Carbon weight loss normalized to the total carbon weight loss and carbon weight loss as found; (right scale) DTG normalized to the total carbon weight loss.

size, adsorbed species, etc., from the same component in the real sample. Furthermore, the embedding degree among the various phases is another crucial factor that cannot be adequately simulated. Looking at Figures 4 and 5 (panel S_1), one can observe that at T_A the MWCNTs are almost absent and at that temperature the carbon weight loss is 86.6%. This fraction is constituted mostly by a graphitic phase, short stubs of MWCNTs, and oxidized catalyst nanoparticles. Short stubs of MWCNTs are no more present in the fraction S_2 at T_B, which is composed only by a graphitic phase and oxidized catalyst nanoparticles. This is confirmed through the feature of graphite at $2\theta = 26.22°$ and the features of the oxidized species of the Nd_2Fe_{17} catalyst as reported in the XRD spectrum of Figure 7.

At T close to T_B, a sharp peak in DTG is present that corresponds in TG to a carbon weight loss change of 3.5% likely attributable to a small fraction of CNTs with homogeneous characteristics.

As already mentioned, the satisfactory resolution of the components in the MWCNT sample of Figure 4 should be attributed to the presence of embedded low quantities of Nd_2Fe_{17} nanoparticles, which properly catalyze the Boudouard reaction. This does not imply that Nd_2Fe_{17} powder could be added as catalyst to a MWCNT sample to perform our TG experiments. In fact, because of the reaction with CO_2, a weight increase of 69.8% is expected if the complete oxidation of Nd_2Fe_{17} occurs. This positive weight change would be superimposed to the carbon weight loss. Furthermore, it is obvious that the contact between the Nd_2Fe_{17} powder and MWCNTs would not be so efficient as expected in the nanostructured configuration.

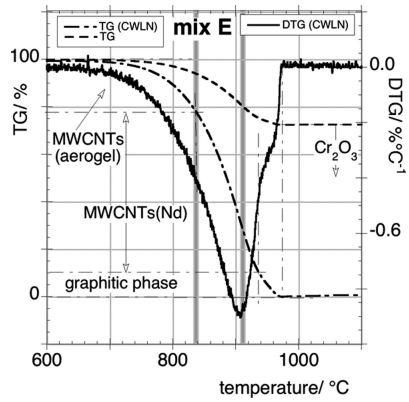

Figure 11. Thermogravimetry of a simulated mixtures composed of two kinds of MWCNTs from $NdNi_5$ and Fe−Co aerogel as respective catalyst at 1 °C min^{-1} in pure CO_2 with catalyst Cr_2O_3. The initial and found compositions are given in Table 2 together with the experimental total carbon weight loss and the weight ratio between catalyst and carbonaceous mixture. The graphic procedure to measure the weight contents is shown by dashed lines. The two vertical grey strips each refer to one to the corresponding DTG minimum of the pure component when tested mixed with Cr_2O_3, as reported in Figure 9. (Left scale) Carbon weight loss normalized (CWLN) to the total carbon weight loss and carbon weight loss as found. (Right scale) DTG normalized (CWLN) to the total carbon weight loss.

According to literature,[9] the ratios I_D/I_G, $I_{G'}/I_G$, and $I_{G'}/I_D$, where I stands for intensity of the D, G, and G′ bands in the Raman spectrum of a carbonaceous sample, are related to its purity in terms of carbon as MWCNTs. The D band is indicative of defects in the MWCNT sample, (i.e., carbonaceous impurities with sp^3 bonding, broken sp^2 bonds in the sidewalls). The G band results from the graphitic nature of the sample (i.e., crystallinity of the sample, pristine arrangement of atoms), and the G′ band is indicative of long-range order in a sample and arises from the two-phonon, second-order scattering process that results in the creation of an inelastic phonon.[36]

The above ratios measured on the spectra of Figure 6 are reported in Table 3, together with the purity calculated according to the relationships given in ref 9. In the same table, the carbon weight loss measured by TG in Figure 4 is given. Considering that the fraction S_0 is constituted by 86.6 wt % MWCNTs (see panel S_0 in Figure 5 and TG curve of Figure 4 at T_A), the values of the calculated purities in Table 3 do not agree with the experimental ones, especially for S_1 and S_2 fractions. The G′ band was assumed able to discriminate between graphite and MWCNTs,[9] but it appears to be sample-dependent. Looking at the graphite Raman spectrum (see Figure 6, fraction S_0), the G′ band is positioned at 2680 (2715) and 2695 (2738) cm^{-1}, respectively, for MWCNTs and graphite. The values in brackets are the wavenumber values of the G′ band given in the above reference. On the other hand, the right position of the N_2 peak excludes any instrumental shift in the wavenumber scale. This behavior is also confirmed[29] by the position of G′ band for MWCNTs grown on $NdNi_5$ (2693 cm^{-1}) and Fe−Co aerogel (2701 cm^{-1}) catalysts. If the same procedure[9] were applied to the graphite Raman spectrum (see Figure 6, fraction S_0), the result would be a sample containing 90 w% of MWCNTs (see Table 3). The features other than D, G, and G′ bands should be attributed to the oxidation products of Nd_2Fe_{17} catalyst.

It is interesting to discuss the behavior of the Boudouard reaction when the carbonaceous mixture is thoroughly mixed with NiO as given in Figure 8. The CWLN curve shows at 900 °C a negative minimum that corresponds exactly to the weight of oxygen contained in the NiO dispersed in the sample. This implies clearly the complete reduction of NiO to Ni. The weight loss centered at 752 °C (see inset in Figure 8B) is so abrupt that it is expected that NiO acts as a true reagent instead of as catalyst. On a thermodynamic basis, the solid-state reactions

$$\mathrm{NiO(s)} + \mathrm{C} = \mathrm{Ni(s)} + \mathrm{CO(g)} \quad (2)$$

and

$$_2\mathrm{NiO(s)} + \mathrm{C} = \mathrm{Ni(s)} + \mathrm{CO2(g)} \quad (3)$$

could occur. Reaction 2 becomes favored starting from 717 K whereas reaction 3 is favored in the full operating range of temperature.[16] The combination of reaction 1 with the Boudouard reaction gives reaction 3. Since the experiments are carried out in pure CO_2, it is expected that for law mass action reasons, reaction 1 is strongly hindered. Just Ni is formed, the reaction

$$\mathrm{Ni(s)} + \mathrm{CO_2(g)} = \mathrm{NiO(s)} + \mathrm{CO(g)} \quad (4)$$

which restores the initial weight of NiO, takes place provided the ratio $pCO/pCO_2 < 6.5 \times 10^{-3}$ at 1173 K. This condition is likely satisfied in a stream of pure CO_2.

By inspection of Figure 9, one observes that with the exception of activated carbon, all the tested carbonaceous materials show the DTG peak positioned at higher temperatures when they are mixed with Cr_2O_3. The difference is large for the two tested samples of MWCNTs (∼100 °C), just 40 °C for graphite and −23 °C for activated carbon. This behavior could be explained in terms of the effectiveness of the contact between the mixed powders. Activated carbon used in this work has a surface specific area of ∼1000 m^2g^{-1}; this large value ensures an intimate contact of the catalyst with the activated carbon powder. Graphite tends to adhere to other materials, whereas MWCNTs do not wet. Although that, the catalyst effectiveness is maintained as demonstrated by the DTG feature at 925 and 939 °C, respectively, for MWCNTs (aerogel) and MWCNTs ($NdNi_5$), which display the presence of another component undetectable without catalyst.

The TG and DTG curves displayed in Figure 10 of simulated mixtures composed by active carbon, MWCNTs ($NdNi_5$), and graphite have been utilized to check the effectiveness of Cr_2O_3 to distinguish and quantify each carbonaceous phase. Table 2 compares the given weight content of each phase with that one found experimentally. In each panel of Figure 10, the graphic procedure to measure the weight contents is shown by dashed lines. In the same figure, three vertical grey strips are plotted each one corresponding to the DTG minimum of the pure component when tested mixed with Cr_2O_3, as reported in Figure 9. In the case of the mixtures, the position in the temperature scale of the corresponding DTG minima is different. It is evident that a certain degree of convolution exists even if the

(36) Saito, R.; Grüneis, A.; Samsonidze, Ge. G.; Brar, V. W.; Dresselhaus, G.; Dresselhaus, M. S.; Jorio, A.; Cançado, L. G.; Fantini, C.; Pimenta, M.; Souza Filho, A. G. *New J. Phys.* **2003**, *5*, 157.

Table 2. Initial and Found Compositions of the Mixtures in Figures 10 and 11 (Cr_2O_3 is the catalyst)

mixture		activated C (%)	MWCNTs[a] (%)	MWCNTs[b] (%)	graphite (%)	$W_{catalyst}/W_{total\ carbon}$	C weight loss (%)
A	given	31.9	21.3		46.8	2.6	26.5
	found	31.6	21.0		47.4		
B	given	33.3	33.3		33.3	3.0	25.5
	found	35.4	30.5		34.0		
C	given	11.8	81.0		7.2	2.5	27.5
	found	11.3	82.3		6.3		
D	given	6.5	79.3		14.2	2.5	27.7
	found	7.2	80.5		12.3		
average relative error (%)		3.0	−1.7		−5.6		
E[c]	given		71.8	28.2		3.6	27.6
	found		67.3	22.4	10.3		

[a] Synthesized by $NdNi_5$ catalyst.[8] [b] Synthesized by Fe−Co catalyst dispersed in aerogel.[27] [c] Figure 11.

presence of Cr_2O_3 gives a decisive contribution to the separation. All the efforts performed to deconvolute the DTG curves did not give satisfactory results, mostly because of the numerical procedures that need to arbitrarily impose the peak fitting and baseline parameters. The graphical procedure displayed in Figure 10 gave the best matching between the expected and found data. As shown in Table 2, the average relative error is within ± 6%.

The evaluation through Figure 11 of a simulated mixture composed by two kinds of MWCNTs gave weight contents lower than expected. The evidence for another graphite-like phase that is close to 10 wt % is displayed. This agrees well with the point outlined before about the presence of another phase in the DTG curves of MWCNTs (aerogel) and MWCNTs ($NdNi_5$) (see respective panels in Figure 9). Both kinds of MWCNTs have the same phase but in different proportion from that which appears as a whole in Figure 11 at temperatures with graphite.

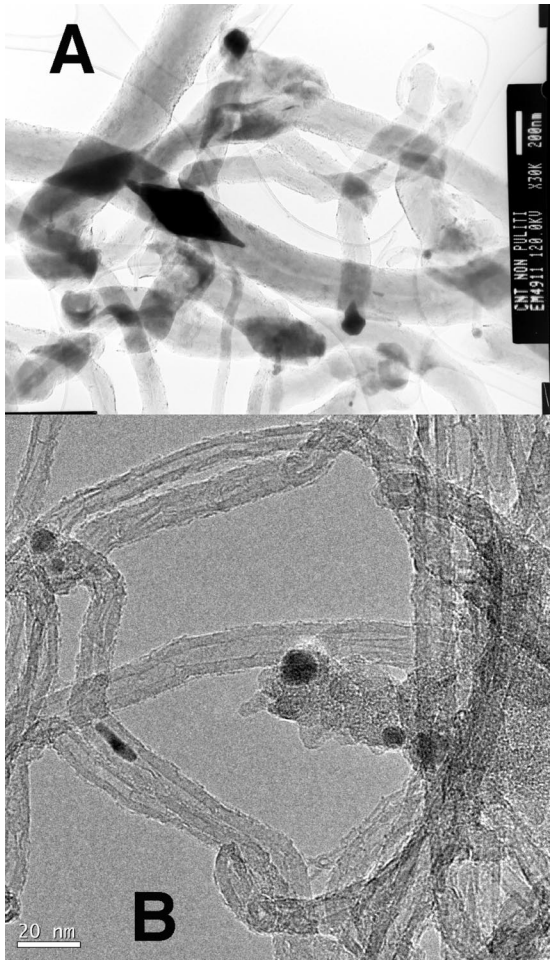

Figure 12. TEM photos of the two kinds of MWCNTs used in the present work. (A) MWCNTs grown on $NdNi_5$[8] as catalyst. (B) MWCNTs grown on Fe−Co aerogel[27] as catalyst.

Table 3. Ratios of the Band Intensities of Raman Spectra of Figure 6

	I_D/I_G	$I_{G'}/I_G$	$I_{G'}/I_D$	C weight loss (%) (Figure 4)
S_0	0.52	0.68	1.30	
calcd purity %	67	78	68	
S_1	0.49	0.80	1.62	86.6
calcd purity %	71	104	79	
S_2	0.30	0.62	2.07	92.8
calcd purity %	100	64	90	
graphite (nuclear grade)	0.28	0.65	2.29	97.0[a]
calcd purity %	103	71	95	90[b]

[a] Figure 9. Calculated purities computed according to the relationships in ref.[9] [b] As average value of the three ratios.

Conclusions

This work gives a contribution to the determination of CNTs in a carbonaceous matrix through use of thermogravimetry under the operating conditions of the Boudouard reaction catalyzed by Cr_2O_3. The results obtained should be considered an effective improvement with respect to the previous efforts reported in the literature to give solution to the problem of checking the CNT purity. The thermogravimetry carried out in pure O_2 or in pure CO_2 as well as the Raman spectroscopy per se cannot guarantee reliable results. The way undertaken in this work to perform thermogravimetry of a carbonaceous sample mixed with a suitable catalyst in a pure CO_2 atmosphere is more promising. Further work should be done to improve the selectivity by looking for catalysts more effective than Cr_2O_3. A tentative rule to look for other suitable catalysts is to test oxides having the following features: (i) values of the free energy change of formation per mol of O_2, at operative temperatures, comparable with the values of Cr_2O_3; (ii) metal characterized by mobile valence; (iii) no change of the oxide stoichiometry, i.e., at the end of reaction, the oxide retains the initial stoichiometry. Cerium oxide (CeO_2), for example, matches this rule.

Acknowledgment. Authors are indebted to Prof. A. Corrias and her group for supplying samples of Fe−Co aerogel catalysts and HRTEM analyses performed on MWCNTs synthesized by the authors by making use of those catalysts.

CM800484J